




OPEN ACCESS

Original research

Metabolic brain networks in dementia with Lewy bodies: from prodromal to manifest disease stages

Matej Perovnik ^{1,2,3}, Urban Simončič⁴, Jan Jamšek⁵, Milica Gregorič Kramberger^{1,3,6}, Joachim Brumberg ^{7,8}, Philipp Tobias Meyer^{7,8}, Daniela Perani⁹, Silvia Paola Caminiti¹⁰, Matthias Brendel^{11,12,13}, Anna Christina Stockbauer^{13,14}, Valle Camacho ¹⁵, Daniel Alcolea ¹⁶, Rik Vandenberghe ¹⁷, Koen Van Laere¹⁸, Ji Hyun Ko¹⁹, Chong Sik Lee²⁰, Matteo Pardini²¹, Lorenzo Lombardo²¹, Alessandro Padovani^{22,23}, Andrea Pilotto ^{22,23}, Miguel A Ochoa-Figueroa²⁴, Anette Davidsson²⁴, Consuelo Cháfer-Pericás²⁵, Lourdes Álvarez-Sánchez²⁵, Valentina Garibotto ^{26,27}, Afina W Lemstra²⁸, Daniel Ferreira^{6,29}, Silvia Daniela Morbelli^{30,31}, Chris C Tang², David Eidelberg², Maja Trošt^{1,3,5}, Alzheimer's Disease Neuroimaging Initiative

► Additional supplemental material is published online only. To view, please visit the journal online (<https://doi.org/10.1136/jnnp-2025-336935>).

For numbered affiliations see end of article.

Correspondence to

Dr Matej Perovnik; matej.perovnik@kclj.si

Received 10 June 2025
Accepted 26 October 2025
Published Online First 4 December 2025



© Author(s) (or their employer(s)) 2026. Re-use permitted under CC BY-NC. No commercial re-use. See rights and permissions. Published by BMJ Group.

To cite: Perovnik M, Simončič U, Jamšek J, et al. *J Neurol Neurosurg Psychiatry* 2026;**97**:316–324.

ABSTRACT

Background Dementia with Lewy bodies (DLB) is the second most common neurodegenerative dementia, yet it remains under-recognised and misdiagnosed, which delays treatment, causes inaccurate prognosis and limits research opportunities. Imaging with 2-[¹⁸F]fluoro-2-deoxy-D-glucose positron emission tomography (FDG PET) is a supportive DLB biomarker. We evaluated a multivariate, quantifiable metabolic network biomarker, termed DLB-related pattern (DLBRP), for its further clinical translation across centres and disease stages.

Methods We analysed demographic, clinical and FDG PET imaging data of 1180 participants from 14 tertiary centres and two multicentre datasets. We included 379 DLB, 28 mild cognitive impairment-LB (MCI-LB), 195 dementia due to Alzheimer's disease (ADD), 172 MCI-AD without α -synuclein co-pathology (MCI-AD-S-), and 73 MCI-AD with α -synuclein co-pathology (S+) patients, along with a comparative group of 333 normal controls (NCs). From the scans, we calculated the expression of DLBRP, AD-related pattern (ADRP) and Parkinson's disease-related pattern (PDRP) and compared them across groups. DLBRP scores were correlated with clinical measurements.

Results Across independent cohorts, DLBRP robustly distinguished DLB from NCs (sensitivity >89%, specificity >90%), and scores correlated with Unified Parkinson's Disease Rating Scale Part III and independently predicted Mini-Mental State Examination. DLBRP was elevated already in MCI-LB. In a small longitudinal dataset, we observed steady increases in DLBRP expression with scores exceeding the diagnostic threshold prior to dementia onset. DLBRP and PDRP discriminated DLB from ADD (sensitivity, 74%–90%; specificity, 80%). In MCI-AD groups, ADRP was expressed, whereas DLBRP and PDRP were increased only in MCI-AD-S+, although comparatively less than in MCI-LB.

Conclusions This study demonstrates the value of DLBRP in diagnosing prodromal and manifest DLB and distinguishing them from their AD counterparts. While overlap between patterns may reflect actual co-

WHAT IS ALREADY KNOWN ON THIS TOPIC

⇒ Imaging with 2-[¹⁸F]fluoro-2-deoxy-D-glucose positron emission tomography supports the diagnosis of dementia with Lewy bodies (DLB), but visual reads are prone to subjectivity; multivariate metabolic-network-based biomarkers, such as DLB-related pattern (DLBRP), Alzheimer disease-related pattern and Parkinson disease-related pattern (PDRP), allow objective, individual-level quantification.

WHAT THIS STUDY ADDS

⇒ In this large observational, multicentre study, DLBRP was validated across 1180 participants, showing robust accuracy for distinguishing DLB patients from controls and Alzheimer dementia patients, and for detecting changes already in prodromal disease. PDRP offers additional complementary diagnostic value.

HOW THIS STUDY MIGHT AFFECT RESEARCH, PRACTICE OR POLICY

⇒ These findings support the use of these novel metabolic brain imaging biomarkers in clinical and research settings for diagnosis and tracking disease progression in prodromal and manifest DLB.

pathology, this possibility cannot be accepted without thorough pathological confirmation. The current findings support the use of DLBRP in patient evaluation and in future trial design.

BACKGROUND

Dementia with Lewy bodies (DLB) is the second most common neurodegenerative dementia, characterised by the presence of cognitive decline, Parkinsonism, visual hallucinations, fluctuating cognition and Rapid Eye Movement (REM) sleep behaviour disorder

(RBD).¹ DLB shares clinical, imaging and pathological similarities with Alzheimer disease dementia (ADD). Despite recent refinement of the diagnostic criteria, DLB remains underdiagnosed.² Patients with DLB are often diagnosed with a delay, undergo more scans and have more alternative prior diagnoses than patients with non-DLB dementias.³ Misdiagnosis can lead to inaccurate therapeutic management, especially in the context of increased sensitivity to antipsychotics, inaccurate prognosis and limited research opportunities.^{1 4 5} Early diagnosis is even more challenging. Recently, the criteria for diagnosing a prodromal stage of DLB, where mild cognitive impairment with LB (MCI-LB) is the most common form, were proposed and validated.^{6 7} MCI-LB shares clinical characteristics with MCI due to AD (MCI-AD), and there is a substantial effect of co-pathologies, with amyloid depositions found in 40% of MCI-LB patients and α -synuclein pathology in 25% of MCI-AD.⁸⁻¹⁰ Common co-pathologies further increase the complexity of the diagnosis and limit research and clinical trials opportunities for these patients.⁴

Metabolic brain imaging with 2-[¹⁸F]fluoro-2-deoxy-D-glucose positron emission tomography (FDG PET) is one of the supportive biomarkers of DLB and MCI-LB.^{1 4 7} Occipital hypometabolism with relatively preserved activity in the temporal lobes, and the appearance of the so-called cingulate island sign (ie, relatively preserved activity in the posterior cingulate cortex) is commonly observed in patients with DLB.¹¹ Similarly, reduced metabolic activity in the occipital lobes is seen in MCI-LB.⁶ However, the inability to accurately detect early, subtle changes in regional metabolism and low inter-rater reliability limit the utility of this neuroimaging sign.^{12 13} Advances in network imaging, such as spatial covariance analysis using a scaled subprofile model/principal component analysis, can further improve the diagnostic value of metabolic brain imaging.^{14 15} Characteristic disease-related metabolic brain patterns, whose expressions can be quantified at an individual patient level, have been identified for many neurodegenerative disorders, including AD (AD-related pattern, ADRP),^{16 17} Parkinson's disease (PD-related pattern, PDRP),^{15 18} and, more recently, DLB.^{15 19} PDRP is characterised by bilateral hypermetabolic changes in the basal ganglia, and hypometabolism in premotor and parietal association cortices. When evaluated

alongside metabolic brain patterns of other atypical Parkinsonian syndromes, PDRP achieved a pooled sensitivity of 84% and specificity of 96% for differentiating PD from multiple system atrophy and progressive supranuclear palsy.²⁰ However, its potential role in distinguishing DLB from ADD has not yet been systematically investigated. DLB-related pattern (DLBRP) was characterised by reduced bilateral metabolic activity in the occipital, posteroinferior parietal and inferior temporal cortices and precuneus, which covaried with relatively increased metabolic activity in the basal ganglia, medial temporal lobes and cerebellum.¹⁹ While it was shown previously that DLBRP captures both α -synuclein and amyloid- β co-pathology and topographically overlaps with both PDRP and ADRP, it is also characterised by metabolic changes specific to DLB.¹⁹ It is not known if DLBRP topography is readily transferable across sites, nor if the pattern is already expressed in prodromal disease. This is critical before a possible clinical integration.²¹

This study had two main and one exploratory specific aim: (1) to study the ability of DLBRP as well as ADRP and PDRP in distinguishing DLB from normal controls (NCs) and ADD; (2) to examine the expression levels for these disease networks in patients with MCI-LB and MCI-AD without (S-) or with (S+) α -synuclein co-pathology and (3) to explore the changes in the expression of DLBRP over time in patients with prodromal and manifest DLB.

METHODS

Participants and procedures

We analysed the demographic, clinical and FDG PET imaging data of 1180 participants from 14 sites and two datasets (table 1). There were 379 DLB, 28 MCI-LB, 195 ADD, 172 MCI-AD-S- and 73 MCI-AD-S+ patients, along with a comparative group of 333 NCs.

Patients with a possible or probable DLB diagnosis were included.^{1 22} For DLB patients, we gathered information on the presence of core features before or at the time of imaging according to diagnostic criteria,¹ the current use of levodopa and antedementia (either acetylcholinesterase inhibitors or NMDA receptor antagonist) medications, and the on-site visual reading of dopamine transporter single-photon emission CT (DAT SPECT), that

Table 1 Demographic and clinical data

Centre	Identification and internal validation			External single-centre testing		External multicentre testing					
	Ljubljana			Seoul		ADNI, AIMN	E-DLB, Freiburg, Milan	E-DLB, Ljubljana	ADNI		
Dg	NC	DLB	ADD	NC	DLB	NC	DLB	MCI-LB	ADD	MCI-AD-S-	MCI-AD-S+
N	74	102	45	16	9	243	268	28	150	172	73
Age (years)	67.0±6.8	75.0±6.7	74.2±7.1	58.4±6.1	72±4.4	68.6±9.8	72.8±7.3	74.8±6.5	74.2±8.1	73.6±6.4	73.6±6.8
MMSE	29.1±0.9	21.3±4.8	18.9±4.9	–	18.6±6	28.9±1.4	21.8±4.6	26.2±2.9	23.3±2.1	27.3±2.1	26.6±2.1
MOCA	26.8±1.9	17.4±5.3	17.4±5.5	–	–	–	21.2±4.8	–	16.8±4.7	22.5±2.9	21.4±2.6
UPDRS	–	–	–	–	35.8±14.3	–	24.5±11.7	15.1±9.8	–	–	–
Dis. dur.	–	3.6±2.0	4±2.5	–	6.7±1.5	–	2.3±1.7	–	–	–	–
Sex (f)	62%	31%	56%	81%	67%	51%	38%	43%	42%	–	–
Park.	–	100%	–	–	–	–	84%	89%	–	–	–
VH	–	73%	–	–	–	–	60%	32%	–	–	–
FC	–	48%	–	–	–	–	56%	59%	–	–	–
RBD	–	46%	–	–	–	–	47%	67%	–	–	–
DaT SPECT (abn)	–	90%	–	–	–	–	89%	82%	–	–	–
Amy (pos)	–	24%	100%	–	–	0%	50%	52%	100%	100%	100%

The data are given as average±SD.

abn, abnormal; AD, Alzheimer disease; ADD, Alzheimer disease dementia; ADNI, Alzheimer's Disease Neuroimaging Initiative; AIMN, Associazione Italiana Medicina Nucleare; Amy, amyloid; DaT SPECT, dopamine transporter imaging with single photon emission CT; Dg, diagnosis; Dis. dur., disease duration; DLB, dementia with Lewy bodies; E-DLB, European DLB consortium; f, female; FC, fluctuating cognition; LB, Lewy body; MCI, mild cognitive impairment; MMSE, Mini-Mental State Examination; MOCA, Montreal Cognitive Assessment; N, number; NC, normal control; Park., parkinsonism; pos, positivity; RBD, Rapid Eye Movement sleep behavior disorder; S, α -synuclein; UPDRS-III, Unified Parkinson Disease Rating Scale; VH, visual hallucinations.

is, either normal or abnormal. Patients with MCI-LB were diagnosed according to the current research guidelines.⁷ Only patients with a characteristic 'Alzheimer' cerebrospinal fluid (CSF) profile were included in the ADD and MCI-AD groups. The MCI-AD group was further divided based on the α -synuclein seed amplification assay results into S- and S+ subgroups.²³ Additionally, we retrospectively identified 8 DLB patients who were scanned twice from the Ljubljana cohort, and we studied the progression of their metabolic brain changes over time (see online supplemental Results). Details of individual cohorts are available in the online supplemental material and elsewhere.^{17 19 24-30}

Amyloid biomarker analysis was performed in 691 individuals, either by CSF analysis or amyloid PET (online supplemental material for further details). FDG PET images were obtained using different scanners (see online supplemental material for further details); however, all scans underwent the same pre-processing steps using an in-house pipeline to preprocess the scans.¹⁷ Each scan was visually checked for quality and adherence to the European Association of Nuclear Medicine (EANM) procedural guidelines to ensure comparability.³¹

Then, we used the forward application routine in ScAnVP software (Center for Neuroscience, Feinstein Institutes for Medical Research, New York, USA, available at: <https://feinsteinneuroscience.org/>)¹⁴ to calculate the expression of previously identified and locally validated DLBRP.¹⁹ We also assessed the expression of previously identified and validated ADRP^{16 17} and PDRP.^{15 18} The resulting raw expression scores were standardised (z -scoring) using local NCs (Ljubljana, Seoul and ADNI) or a large combined cohort from ADNI and AIMN (European DLB Consortium, Milan and Freiburg). Patients and NCs from Ljubljana, not used for the identification and initial validation of the DLBRP,¹⁹ were deemed the second internal validation group. Patients and NCs from Seoul were considered the external single-centre testing group, as this was the only cohort with local NC scans.

Statistical methods

Student's independent-sample t -test, one-way analysis of variance with post hoc Tukey HSD or χ^2 test were used to compare demographic data across groups, as appropriate. One-way ANCOVA with post hoc Tukey HSD (family-wise error within model) was used to assess group differences in pattern expression while controlling for scanner and, when needed, for the confounding effects of age and sex. Furthermore, due to the spatial overlap between DLBRP, PDRP and ADRP, which could lead to non-specific elevation of subject scores,^{16 19} we included the subject scores of DLBRP, PDRP or ADRP as covariates in our analysis, as appropriate. A student paired t -test was used to assess within-group differences in network expression.

The p ROC package³² was used to calculate the area under the curve (AUC). Specificity and sensitivity values were determined using Youden's index, first calculated from the first internal validation group (21 NCs and 59 DLB)¹⁹ and then from the current dataset. Variability in the AUC, specificity and sensitivity was estimated by bootstrap resampling with 1000 iterations. Pearson's correlation coefficient was used for simple correlational analyses between pattern scores and Mini-Mental State Examination (MMSE) and Unified Parkinson's Disease Rating Scale Part III (UPDRS-III). Then, multivariate linear regression models and/or partial correlation analyses were conducted to assess the relationship between subject scores and cognitive and motor impairment. Variance inflation factor (VIF) was calculated to assess the severity of multicollinearity in the regression models (see online supplemental material for further details). False discovery rate (FDR) corrected p values using the Benjamini-Hochberg approach are reported.

All statistical analyses were conducted in RStudio V.2024.4.2.764,³³ R V.4.4.1³⁴ and figures were produced with the *ggplot2* package.³⁵ Results were considered significant at $p < 0.05$ (two-tailed).

RESULTS

Demographic and clinical data are presented in [table 1](#).

DLBRP expression in patients with DLB and NCs

Comparisons between identification and first internal validation of DLB and NC cohorts have been reported previously.¹⁹ The optimal (general) threshold was derived from the first internal validation group and set at $Z = 1.43$, which yielded high sensitivity (93%) and specificity (100%) with an AUC of 0.99.

Internal single-centre validation

The second internal validation group consisted of 33 NCs and 23 DLB. NCs were younger ($p=0.01$), had a higher proportion of females ($p = 0.01$) and had higher MMSE scores ($p < 0.001$) than DLB. The DLB group had higher, adjusted for age and sex, DLBRP expression than the NCs (difference = 4.6, $p < 0.001$, [figure 1A](#)), which enabled high discrimination accuracy with general ([table 2](#)) or dataset-specific (online supplemental table 1) thresholds.

External single-centre testing

Patients and NCs from Seoul were considered an external single-centre testing cohort. The NCs were younger than the DLB ($p < 0.001$), but the groups did not differ in sex distribution ($p = 0.74$). The DLB had higher, adjusted for age, DLBRP expression than the NCs (difference = 4.02, $p = 0.0005$, [figure 1A](#)), which enabled high discrimination accuracy with general ([table 2](#)) or dataset-specific (online supplemental table 1) thresholds.

External multicentre testing

The 243 NCs from the ADNI and AIMN databases and 268 patients from the European DLB consortium, Freiburg and Milan, comprised the external multicentre testing group. NCs were younger ($p < 0.001$), had a higher proportion of females ($p = 0.004$) and had higher MMSE scores ($p < 0.001$) than DLB. The DLB had higher, adjusted for scanner, age and sex, DLBRP expression than the NCs (difference = 4.69, $p < 0.001$, [figure 1A](#)), which enabled high discrimination accuracy with general ([table 2](#)) or dataset-specific (online supplemental table 1) thresholds.

Relationship between metabolic brain networks and clinical features

Core features, cognition and treatment

DLB and MCI-LB groups were combined to study the relationship between metabolic network expression and clinical features. We observed a significant correlation between UPDRS-III and DLBRP expression ($p_{\text{FDR}} = 0.04$) and a non-significant trend for PDRP ($p_{\text{FDR}} = 0.07$). High collinearity was noted between the DLBRP and PDRP scores (VIFs > 13); therefore, only a partial correlation analysis was performed. The covariate-adjusted correlation between DLBRP expression and UDRPS-III was significant ($r = 0.26$ (0.05, 0.45), $p_{\text{FDR}} = 0.04$, [figure 1B](#)), but not between PDRP and UPDRS-III ($r = 0.20$ (-0.02, 0.40), $p_{\text{FDR}} = 0.07$).

We observed a significant correlation between MMSE and DLBRP ($p_{\text{FDR}} < 0.001$) and ADRP ($p_{\text{FDR}} < 0.001$). A covariate-adjusted multivariate linear regression model showed significant contributions of DLBRP ($\beta = -0.55$ (-0.80, -0.30), p_{FDR}

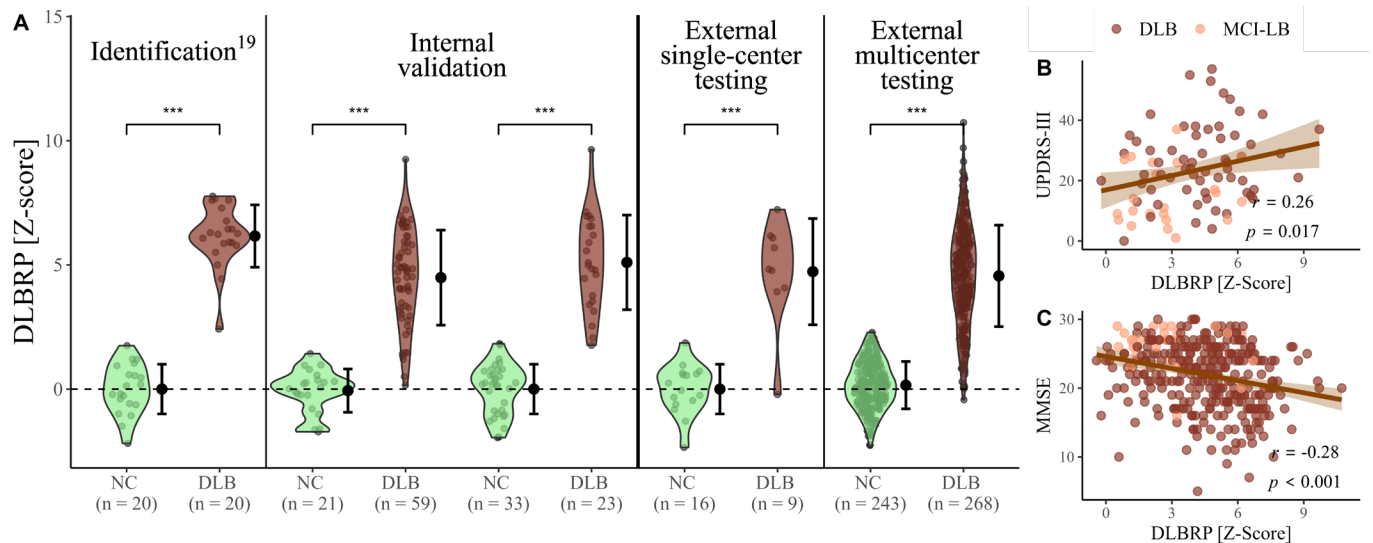


Figure 1 Dementia with Lewy bodies-related pattern (DLBRP) expression across sites and correlations with motor and cognitive impairment. (A) Expression of DLBRP in patients with DLB and normal controls (NCs). Data are Z-transformed (see Methods). Means and SDs are presented to the right of individual data points. Identification—patients and NCs used to derive DLBRP¹⁹; and correlation between DLBRP and (B) Unified Parkinson's Disease Rating Scale-Part III (UPDRS-III) and (C) Mini-Mental State Examination (MMSE). Partial correlation coefficients adjusted for age and sex are shown. Internal Validation—patients and NCs from Ljubljana; External single-centre testing—patients and NCs from Seoul; External multicentre testing—patients and NCs from the European DLB consortium, Freiburg, Milan, Alzheimer's disease Neuroimaging Initiative and Associazione Italiana Medicina Nucleare database. *** $p < 0.001$. MCI-LB, mild cognitive impairment with LB.

< 0.001) and ADRP ($\beta = -0.50$ ($-0.78, -0.22$), $p_{\text{FDR}} < 0.001$) to MMSE. The covariate-adjusted partial correlation analysis showed a significant correlation between DLBRP and MMSE ($r = -0.28$ ($-0.38, -0.18$), $p_{\text{FDR}} < 0.001$, **figure 1C**), and between ADRP and MMSE ($r = -0.24$ ($-0.34, -0.14$), $p_{\text{FDR}} < 0.001$).

After adjusting for confounding variables, DLBRP expression did not differ according to the presence or absence of each core clinical feature or current treatment status (online supplemental table 2).

DAT imaging (DAT SPECT)

There was no difference in age ($p = 0.95$), sex ($p = 0.41$) or MMSE ($p = 0.89$) between patients with ($n = 162$) and without ($n = 20$) dopaminergic loss. Patients with reduced DAT density in the basal ganglia had higher DLBRP expression than those with normal dopaminergic integrity ($p = 0.003$).

Metabolic brain networks in DLB and ADD

Internal single-centre validation

The 82 DLB and 45 ADD patients from Ljubljana comprised the internal validation set. The DLB group was predominantly male ($p = 0.02$) with higher MMSE scores ($p = 0.005$). The covariate-adjusted expressions of DLBRP, ADRP and PDRP differed between the groups (all $p < 0.001$, (online supplemental figure 1).

Moderate discrimination was observed between DLB and ADD based on DLBRP ($AUC = 0.78$), ADRP ($AUC = 0.66$) and PDRP ($AUC = 0.76$) expression, with moderate sensitivity for DLBRP (74%) and PDRP (74%), but not for ADRP (48%). All patterns achieved good specificity (76%–82%), using a general (online supplemental table 3A) or an optimal threshold from the external multicentre validation group (online supplemental table 3B).

External multicentre testing

The external multicentre testing group comprised 277 DLB and 150 ADD patients from the European DLB consortium, Freiburg, Milan, Seoul and ADNI. The DLB group was marginally younger ($p = 0.06$) and had lower MMSE scores ($p < 0.001$). The covariate-adjusted expressions of DLBRP (**figure 2A**), ADRP (**figure 2B**), and PDRP (**figure 2C**) differed between the groups (all $p < 0.01$).

ADRP expression did not discriminate DLB patients from other patient categories ($AUC = 0.54$). However, based on the DLBRP, we could accurately separate the DLB and ADD groups ($AUC = 0.83$) with good sensitivity (75%) and specificity (80%). PDRP, by contrast, showed superior discrimination ($AUC = 0.93$) and sensitivity (90%) with identical specificity (80%) using a general (online supplemental table 3A) or dataset-specific optimal threshold (online supplemental table 3B).

Table 2 Performance metrics with 95% CIs for discrimination between patients with dementia with Lewy bodies (DLB) from normal controls (NCs) based on DLB-related pattern expression scores

Group	DLB vs NC, Z = 1.43			
	First internal validation	Second internal validation	External single-centre testing	External multicentre testing
AUC	0.99 (0.96–1.00)	1.00 (0.99–1.00)	0.94 (0.79–1.00)	0.97 (0.96–0.98)
Sensitivity	0.93 (0.86–0.99)	1.00 (1.00–1.00)	0.89 (0.67–1.00)	0.93 (0.90–0.96)
Specificity	1.00 (1.00–1.00)	0.94 (0.85–1.00)	0.94 (0.80–1.00)	0.90 (0.86–0.93)

AUC, area under the curve.

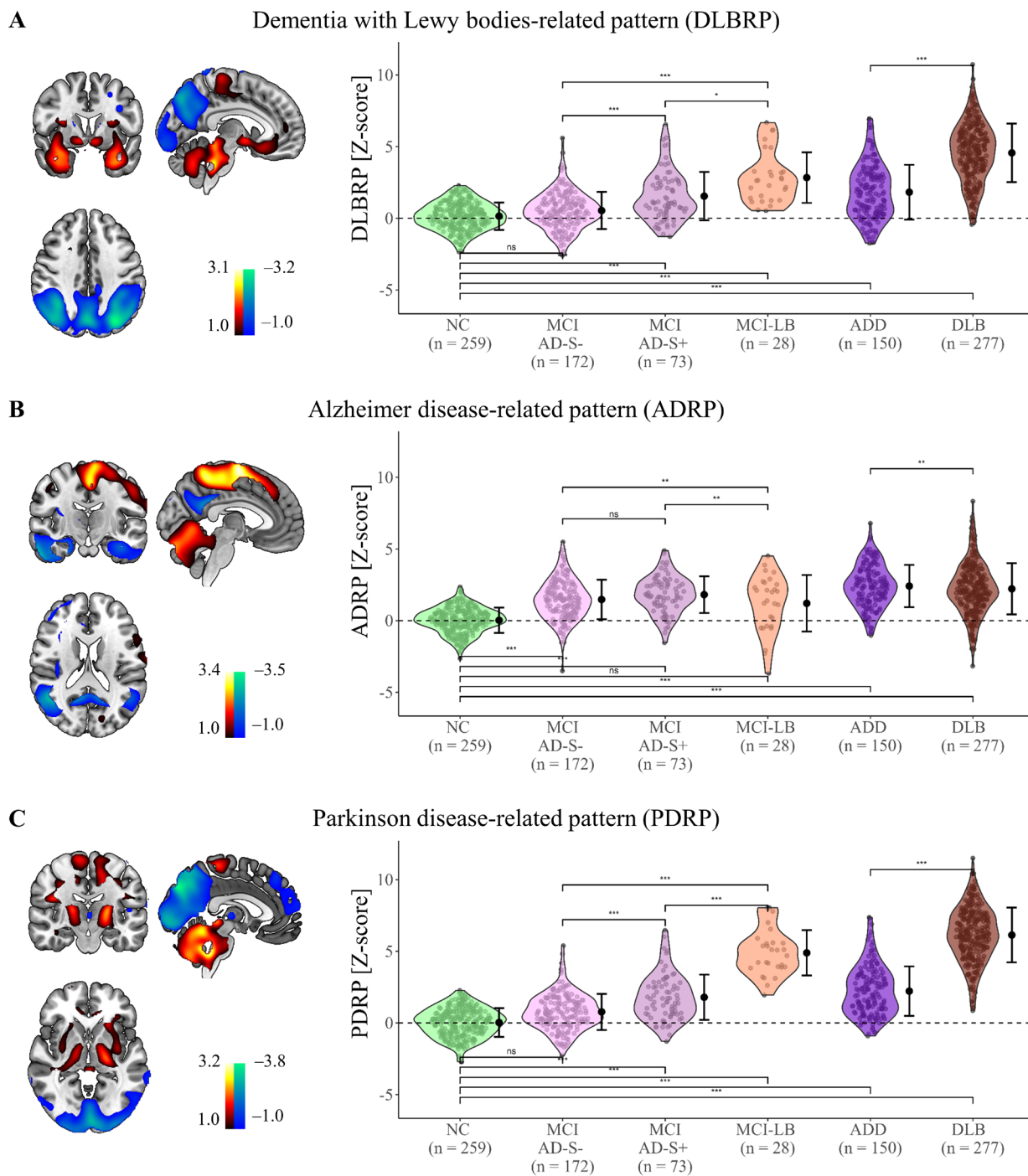


Figure 2 Visualisation of metabolic brain patterns and their expression in patients with prodromal and manifest dementia with Lewy bodies (DLB) and Alzheimer disease dementia (ADD). The visualisation (left) and expression (right) of (A) DLB-related pattern (DLBRP), (B) AD-related pattern (ADRP) and (C) Parkinson disease-related pattern (PDRP) in patients with DLB, ADD, mild cognitive impairment (MCI) and normal controls (NCs). Data are Z-transformed (see Methods). Means and SDs are presented to the right of individual data points. Post hoc comparisons after adjustment for age, sex and confounding pattern expression levels (ie, DLBRP or ADRP) are shown. * $p < 0.05$, ** $p < 0.01$, *** $p < 0.001$, ns, non-significant. AD, Alzheimer disease; DLB, dementia with Lewy bodies; MCI-AD-S-, MCI due to AD without α -synuclein co-pathology; MCI-AD-S+, MCI due to AD with α -synuclein co-pathology; MCI-LB, mild cognitive impairment with Lewy bodies.

Metabolic brain networks in patients with MCI

The MCI groups were younger (all $p < 0.002$), had lower MMSE scores (all $p < 0.001$) and were predominantly male ($p = 0.04$) compared with the NCs. MMSE scores were lower in the MCI-AD-S+ ($p = 0.028$) and MCI-LB ($p = 0.01$) groups than in the MCI-AD-S- group.

The covariate-adjusted mean DLBRP expression was significantly different (all $p < 0.01$) between all comparison pairs, except between MCI-AD-S- and NCs (figure 2A). The covariate-adjusted mean ADRP expression was significantly higher in the MCI-AD group than in the NCs and MCI-LB groups (all $p < 0.01$, figure 2B). The other comparison pairs were not significant

(both $p > 0.90$). The covariate-adjusted mean PDRP expression was significantly different (all $p < 0.001$) between all comparison pairs, except between MCI-AD-S- and NCs (figure 2C). Within-group network differences are reported in the online supplemental material.

DISCUSSION

In this study, we investigated brain metabolic-network biomarkers in a large-scale multicentre cohort of patients with prodromal and manifest DLB and compared them with their AD counterparts and NC subjects with an aim to accelerate the translation of DLBRP into clinical practice to overcome the unmet diagnostic and treatment needs in DLB. We showed that DLBRP is uniformly expressed in patients with DLB across different centres and that DLBRP expression correlates with patients' clinical status. Patients with worse motor and cognitive performances exhibited higher DLBRP expression. Furthermore, we observed an abnormal elevation of DLBRP in prodromal DLB (ie, MCI-LB). In a small longitudinal dataset, we observed steady longitudinal increases in DLBRP expression (online supplemental material). Lastly, a comparison between patients with DLB and ADD and between patients with MCI-LB and MCI-AD showed that DLBRP and PDRP can accurately distinguish these patients, who often present with similar clinical presentations.

We proved that the DLBRP identified in one centre can be reliably applied to the imaging data acquired across different centres and scanners, thus showing its high potential as a metabolic imaging biomarker of DLB.³⁶ Indeed, the optimal threshold, derived from the internal validation group ($Z = 1.43$), showed high specificity ($>90\%$), sensitivity ($>89\%$) and AUCs (>0.94) for the discrimination between DLB and NCs in all analysed groups. Whereas current diagnostic guidelines rely purely on the visual assessment of FDG PET scans,¹ DLBRP is a quantifiable biomarker that can improve metabolic brain imaging performance. We also showed that DLBRP scores correlated with MMSE ($r = -0.31$) and UPDRS-III ($r = 0.24$) scores at a group level. Previous studies reported correlations between DLBRP and MMSE in the range of -0.26 and -0.47 , although in smaller samples ($n = 50-67$) compared with ours ($n = 335$).^{19, 37-39} Moreover, a multivariate analysis showed a significant and independent, although smaller, role of ADRP as an MMSE predictor, highlighting the dual pathology, that is, LB and AD, in DLB. A previous study, however, did not observe a correlation between DLBRP and UPDRS-III.³⁸ This divergent finding may be attributed to differences in sample sizes, biomarker plateauing or specific cohort characteristics, as the latter cohort was more advanced with higher UPDRS-III scores.³⁸

To capture a broader spectrum of the disease, we included prodromal cases in this study. In MCI-LB, we observed elevated DLBRP and PDRP, but normal ADRP scores. While in manifest DLB cases, increased ADRP levels have been consistently reported,^{19, 40} and ADRP contributes to cognitive decline, as seen from our analyses, this is not yet the case in MCI-LB. Here, the DLBRP and PDRP dominate. This is concordant with a regional metabolic analysis that showed more severe metabolic deficits in parietal and occipital regions in MCI patients who progressed to DLB, compared with those who progressed to ADD and had more substantial involvement of the medial temporal lobes and posterior-mid cingulate cortex.⁴¹ Similar regional metabolic changes were reported in MCI-RBD patients.⁴² Both DLBRP and PDRP are characterised by substantial posterior hypometabolism. In our sample, in which the vast majority (89%) of MCI-LB patients had Parkinsonism, PDRP levels were even higher than

those of DLBRP. Metabolic network activity in MCI-LB patients without Parkinsonism and in those with delirium or psychiatric onset remains to be studied. Suprathreshold DLBRP expression was observed before the appearance of dementia in the longitudinal part of the study (see online supplemental material and figure 2). Here, we showed uniform increases in DLBRP levels for all patients, highlighting the progressive nature of network expression, which shows its potential to be used as a biomarker of disease progression. While PDRP scores have been shown to increase over time in patients who convert from RBD to PD,⁴³ this has not yet been shown for RBD to DLB converters. Although occipital hypometabolism has been noted in RBD cases before.⁴⁴ To summarise, we believe that these findings strengthen the rationale of employing the FDG PET-based biomarkers as a surrogate marker in clinical trials of not only manifest but also prodromal DLB.⁴⁵

In patients with MCI-AD, we observed substantially elevated subject scores of DLBRP and PDRP only in the presence of α -synuclein pathology (S+). Interestingly, ADRP scores were elevated to a similar degree in MCI-AD, regardless of the S status. It was shown before that α -synuclein co-pathology exacerbates cognitive decline in MCI-AD patients and contributes to a more prominent posterior hypometabolism.⁸ A direct longitudinal comparison between MCI-LB and MCI-AD groups remains to be studied.

Finally, to study the differential diagnostic value of DLBRP and other metabolic brain networks, we compared patients with prodromal and manifest DLB with their AD counterparts. DLBRP (AUC=0.84) and PDRP (AUC = 0.94) enable accurate discrimination between DLB and ADD, with superior sensitivity for PDRP (74% vs 91%) and the same specificity (80%). The majority of our DLB patients had Parkinsonism, which may drive the superior discriminative PDRP performance, whereas DLBRP may be particularly informative when Parkinsonism is absent or mild.⁴⁶ In clinical practice, a single FDG PET scan can be used to assess the presence of several disease-related networks simultaneously, that is, the calculation of DLBRP, PDRP and ADRP expressions is easily performed for each patient.¹⁵ Indeed, classification algorithms that are based on several disease-related networks have been shown to improve diagnostic accuracy in neurodegenerative dementias¹³ and Parkinsonian disorders.^{15, 47} These are being extended to include DLBRP.

ADD patients exhibit elevated levels of DLBRP, and DLB patients exhibit elevated levels of ADRP, explained largely by the spatial overlap between the patterns and the neuropathological overlap between AD and DLB.¹⁹ While there is a spatial overlap between ADRP and PDRP with non-specific elevations in PD and ADD patients, respectively, this is comparatively smaller.^{16, 19} PDRP likely reflects neurodegeneration predominantly caused by the LB pathology, whereas DLBRP may represent the manifestation of both LB and AD pathologies. Topographically, DLBRP comprises occipital and posterior temporoparietal hypometabolism that extends into the middle and inferior temporal gyri, overlapping with ADRP. By contrast, relative increases in the basal ganglia are characteristic of both DLBRP and PDRP. The topographic differences are in line with pathological studies that show the distinction between DLB and PDD, supporting the need for a specific DLB imaging biomarker.⁴⁸ Similarly, pathological studies show a more common AD co-pathology in DLB compared with the presence of LB co-pathology in ADD⁴⁹; however, AD pathology is less pronounced in DLB than in ADD.⁵⁰ Only MCI-AD-S+ individuals had substantially elevated subject scores of DLBRP and PDRP. As expected, the ADRP scores were elevated to a

similar degree in all patients with MCI-AD, regardless of their α -synuclein status.

Because NCs were younger than the patient groups, analyses were age-adjusted. DLBRP scores correlated weakly with age in NCs ($r = 0.12$, $p = 0.03$) and negatively in AD ($r = -0.36$, $p = 0.01$), but not in DLB ($r = -0.04$, $p = 0.47$). Normal ageing is accompanied by metabolic changes, notably in the anterior cingulate cortex, posterior cingulate cortex and lateral parietal cortex.⁵¹ The weak NC association likely reflects age-related metabolic decline in regions partly overlapping with the DLBRP topography, whereas in DLB, scores appear unaffected by age, consistent with disease-specific changes. In AD, the inverse association may reflect greater disease burden in younger patients, though this requires further study.

Limitations

The absence of concomitant α -synuclein and AD biomarkers in all cohorts and the lack of histopathological confirmation are the main limitations of this study, which may increase the heterogeneity of our sample. However, large cohorts reduce the possible effect of misdiagnosis on the conclusions. Second, the patients were scanned with different scanners, without a strict scanner harmonisation procedure in place; however, the scanner type was accounted for statistically. The retrospective nature and recruitment sites (see online supplemental material) of the current study may have introduced a selection bias, as patients with DLB are more likely to undergo FDG PET imaging if the cognitive deficit is only accompanied by movement disorder symptoms.⁵² This could partly explain the high prevalence of Parkinsonism in our cohort and may limit the generalisability of our findings, as Parkinsonism is less frequent in the broader DLB population.^{53–54} Finally, local NC scans were not always available, which could reduce the reported diagnostic accuracy of DLBRP. We used data from two large cohorts for z-standardisation, instead of a small local NC cohort. Furthermore, pattern scores and performance are largely independent of the PET system^{55–57} or resolution.⁵⁸

CONCLUSIONS

In conclusion, this extensive multicentre study demonstrated the effectiveness of DLBRP, a metabolic-network-based imaging biomarker, in diagnosing patients with both prodromal and manifest DLB across different sites, as well as in differentiating them from their AD counterparts. The observed longitudinal increases in DLBRP scores, along with their correlations with cognitive and motor impairments, indicate the additional value of this biomarker in monitoring disease progression. Moreover, DLBRP expression holds promise as a surrogate marker for disease-modifying treatments.

Author affiliations

¹Department of Neurology, University Medical Centre Ljubljana, Ljubljana, Slovenia

²Feinstein Institutes for Medical Research, Northwell Health, Manhasset, New York, USA

³Faculty of Medicine, University of Ljubljana, Ljubljana, Slovenia

⁴Faculty of Mathematics and Physics, University of Ljubljana, Ljubljana, Slovenia

⁵Department of Nuclear Medicine, University Medical Centre Ljubljana, Ljubljana, Slovenia

⁶Division of Clinical Geriatrics, Center for Alzheimer Research, Department of Neurobiology, Care Sciences and Society, Karolinska Institutet, Stockholm, Sweden

⁷Department of Nuclear Medicine, Medical Center-University of Freiburg, Freiburg, Germany

⁸Faculty of Medicine, University of Freiburg, Freiburg, Germany

⁹Vita-Salute San Raffaele University, Milan, Italy

¹⁰Department of Brain and Behavioral Sciences, University of Pavia, Pavia, Italy

¹¹Department of Nuclear Medicine, LMU Hospital, Munich, Germany

¹²German Centre for Neurodegenerative Diseases, Munich, Germany

¹³Munich Cluster for Systems Neurology (SyNergy), Munich, Germany

¹⁴Department of Neurology, LMU Hospital, Munich, Germany

¹⁵Nuclear Medicine Department, Hospital de la Santa Creu i Sant Pau, Barcelona, Spain

¹⁶Sant Pau Memory Unit, Department of Neurology, Hospital de la Santa Creu i Sant Pau, Barcelona, Spain

¹⁷Laboratory for Cognitive Neurology, Department of Neurosciences, Faculty of Medicine, KU Leuven, Leuven, Belgium

¹⁸Nuclear Medicine and Molecular Imaging, Department of Imaging and Pathology, KU Leuven, Leuven, Belgium

¹⁹Department of Human Anatomy and Cell Science, Rady Faculty of Health Sciences, University of Manitoba, Winnipeg, Manitoba, Canada

²⁰CHA Bundang Medical Center, CHA University, Seongnam-si, Korea (the Republic of)

²¹Department of Neuroscience, University of Genoa, Genova, Italy

²²Department of Clinical and Experimental Sciences, University of Brescia, Brescia, Italy

²³Department of Continuity of Care and Frailty, Unit of Neurology, ASST Spedali Civili di Brescia, Brescia, Italy

²⁴Department of Clinical Physiology, Institution of Medicine and Health Sciences, Linköping University Hospital, Linköping, Sweden

²⁵Alzheimer's Disease Research Group, Instituto de Investigación Sanitaria La Fe, Valencia, Spain

²⁶Division of Nuclear Medicine and Molecular Imaging, Geneva University Hospitals, Geneva, Switzerland

²⁷NIMTlab, Geneva University, Geneva, Switzerland

²⁸Alzheimer Center Amsterdam, Department of Neurology, Amsterdam UMC Locatie De Boelelaan, Amsterdam, The Netherlands

²⁹Facultad de Ciencias de la Salud, Universidad Fernando Pessoa Canarias, Las Palmas de Gran Canaria, Spain

³⁰Department of Medical Sciences, University of Turin, Turin, Italy

³¹Nuclear Medicine Unit, Città della Salute e della Scienza Torino, Turin, Italy

Acknowledgements We wish to thank Ms Hana Kos for her help with data curation. We thank the Italian Association of Nuclear Medicine (AIMN), the following Institutions and researchers for sharing the normal FDG normal dataset: Flavio Nobili and Silvia Morbelli, University of Genoa and IRCCS Ospedale Policlinico San Martino, Genoa; Sabina Pappatà, Institute of Bio-structure and Bioimaging of the CNR and Department of Advanced Biomedical Sciences, Federico II University, Naples; Angelina Cistaro, formerly at the IRMET, Torino, Italy; Duccio Volterrani, Regional Center of Nuclear Medicine, Hospital University of Pisa, Pisa; Valentina Berti, Nuclear Medicine Unit, University of Florence; Maria Lucia Calcagni, Nuclear Medicine Unit, Università Cattolica del Sacro Cuore, Rome; Stelvio Sestini, Nuclear Medicine Unit Santo Stefano Prato Hospital, Prato. We also thank Professor Daniela Perani and Professor Luca Presotto (Vita-Salute San Raffaele University Nuclear Medicine Unit San Raffaele Hospital Division of Neuroscience San Raffaele Scientific Institute Milan) for the fruitful collaboration and for the important work devoted to elaborate FDG data for the database. Finally, we thank Professor Andrea Chincarini (Istituto Nazionale Fisica Nucleare, Genova) for the support in collecting and reviewing PET data.

Collaborators Alzheimer's Disease Neuroimaging Initiative: Part of the data used in this study was obtained from the Alzheimer's Disease Neuroimaging Initiative (ADNI) database (adni.loni.usc.edu). As such, the investigators within the ADNI contributed to the design and implementation of ADNI and/or provided data, but did not participate in the analysis or writing of this report. A complete listing of ADNI investigators can be found at: http://adni.loni.usc.edu/wp-content/uploads/how_to_apply/ADNI_Acknowledgement_List.pdf.

Contributors MPE and MT developed the study concept and design. MPE conducted the data analysis, data curation and drafted the original work. US helped with data curation. MPE, CCT, DE and MT contributed to the interpretation of the data. MPE, MT, JJ, MGK, JB, PTM, DP, SPC, MB, ACS, VC, DA, RV, KVL, JHK, CSL, MPa, LL, APa, API, MAO-F, AD, CC-P, LA-S, VG, AWL, DF and SDM recruited the participants and collected data from different centres. All authors reviewed and revised the final draft. MPE is the guarantor for this manuscript.

Funding This work was supported by the Slovenian Research Agency (ARRS) through grants P1-0389, J3-60059, J7-2600 and J7-3150. MP is a recipient of the Fulbright Visiting Scholar Program sponsored by the US Department of State's Bureau of Educational and Cultural Affairs. JB was supported by the Berta-Ottenstein programprogramme for Advanced Clinician Scientist, Faculty of Medicine, University of Freiburg. MB was funded by the Deutsche Forschungsgemeinschaft (DFG) under Germany's Excellence Strategy within the framework of the Munich Cluster for Systems Neurology (EXC 2145 SyNergy, ID 390857198). DF receives funding from the Swedish Research Council (Vetenskapsrådet, grant 2022-00916), the Center for Innovative Medicine (CIMED, grants 20200505 and FoUI-988826), the regional agreement on medical training and clinical research of Stockholm Region (ALF Medicine, grants FoUI-962240 and FoUI-987534), the Swedish Brain Foundation

(Hjärnfonden FO2023-0261, FO2022-0175, FO2021-0131), the Swedish Alzheimer Foundation (Alzheimerfonden AF-968032, AF-980580, AF-994058), the Swedish Demensia (Alzheimerfonden Demensfonden), the Gamla Tjänarinnor Foundation, the Gun och Bertil Stohnes Foundation, the Åke Wiberg Foundation, StratNeuro, Funding for Research from Karolinska Institutet, Neurofonden and the Foundation for Geriatric Diseases at Karolinska Institutet, as well as contributions from private bequests. Data collection and sharing for this project was funded by the Alzheimer's Disease Neuroimaging Initiative (ADNI) (National Institutes of Health Grant U01 AG024904) and DOD ADNI (Department of Defense award number W81XWH-12-2-0012). ADNI is funded by the National Institute on Aging, the National Institute of Biomedical Imaging and Bioengineering, and through generous contributions from the following: AbbVie, Alzheimer's Association; Alzheimer's Drug Discovery Foundation; Araclon Biotech; BioClinica; Biogen; Bristol-Myers Squibb Company; CereSpir; Cogstate; Eisai; Elan Pharmaceuticals; Eli Lilly and Company; EuroImmun; Hoffmann-La Roche and its affiliated company Genentech; Fujirebio; GE Healthcare; IXICO; Janssen Alzheimer Immunotherapy Research & Development; Johnson & Johnson Pharmaceutical Research & Development; Lumosity; Lundbeck; Merck & Co; Meso Scale Diagnostics; NeuroRx Research; Neurotrack Technologies; Novartis Pharmaceuticals Corporation; Pfizer; Piramal Imaging; Servier; Takeda Pharmaceutical Company and Transition Therapeutics. The Canadian Institutes of Health Research is providing funds to support ADNI clinical sites in Canada. Private sector contributions are facilitated by the Foundation for the National Institutes of Health (www.fnih.org). The grantee organization is the Northern California Institute for Research and Education, and the study is coordinated by the Alzheimer's Therapeutic Research Institute at the University of Southern California. ADNI data are disseminated by the Laboratory for Neuro Imaging at the University of Southern California. The research position of Silvia Paola Caminiti was supported by the Italian Ministry of Health (grant RF-2018-12366209) and by #NEXTGENERATIONEU (NGEU), funded by the Ministry of University and Research (MIUR), NRRP project MNESYS (PE0000006).

Competing interests MB is a member of the Neuroimaging Committee of the EANM. MB has received speaker honoraria from Roche, GE Healthcare, Iba and Life Molecular Imaging; has advised Life Molecular Imaging and GE Healthcare; and is currently on the advisory board of MIAC. DF consults for BioArctic and has received honoraria from Esteve. KVL serves on the advisory board for Enigma and has received speaker honoraria from GE Healthcare. DA participated in advisory boards from Fujirebio-Europe, Roche Diagnostics, Grifols S.A. and Lilly, and received speaker honoraria from Fujirebio-Europe, Roche Diagnostics, Nutricia, Krka Farmaceutična S.L., Zambon S.A.U., Neuraxpharm, Alter Medica, Lilly and Esteve Pharmaceuticals S.A. DA declares a filed patent application (WO2019175379 Markers of synaptopathy in neurodegenerative disease). MPE, US, JJ, MGK, JB, PTM, ACS, VC, RV, JHK, CSL, MPa, LL, APa, APi, MAO-F, AD, CC-P, LA-S, VG, AWL, SDM, CCT, DE and MT declare no conflicts of interest.

Patient consent for publication Not applicable.

Ethics approval This study involves human participants and was approved by the Slovenian National Ethics Committee (0120-584/2019/5). For patients and healthy volunteers participating in ADNI protocols, written informed consent was obtained after approval was granted by the institutional review board of the collaborating institutions. Local institutional ethics committee approvals for the retrospective analyses were available for all other centres, including the transfer of imaging data. Patients gave informed written consent for the imaging procedure and radiopharmaceutical application. Participants gave informed consent to participate in the study before taking part.

Provenance and peer review Not commissioned; externally peer reviewed.

Data availability statement Data are available on reasonable request. Data may be obtained from a third party and are not publicly available. Data from UMC Ljubljana are available on reasonable request. Data from the European DLB consortium and other centres may be obtained from a third party and are not publicly available. Data from the ADNI are available in a public repository. Interested scientists may obtain access to ADNI imaging, clinical, genomic and biomarker data for the purposes of scientific investigation, teaching or planning clinical research studies. Access is contingent on adherence to the ADNI Data Use Agreement and the publication policies.

Supplemental material This content has been supplied by the author(s). It has not been vetted by BMJ Publishing Group Limited (BMJ) and may not have been peer-reviewed. Any opinions or recommendations discussed are solely those of the author(s) and are not endorsed by BMJ. BMJ disclaims all liability and responsibility arising from any reliance placed on the content. Where the content includes any translated material, BMJ does not warrant the accuracy and reliability of the translations (including but not limited to local regulations, clinical guidelines, terminology, drug names and drug dosages), and is not responsible for any error and/or omissions arising from translation and adaptation or otherwise.

Open access This is an open access article distributed in accordance with the Creative Commons Attribution Non Commercial (CC BY-NC 4.0) license, which

permits others to distribute, remix, adapt, build upon this work non-commercially, and license their derivative works on different terms, provided the original work is properly cited, appropriate credit is given, any changes made indicated, and the use is non-commercial. See: <https://creativecommons.org/licenses/by-nc/4.0/>.

ORCID iDs

Matej Perovnik <https://orcid.org/0000-0001-8595-7773>
 Joachim Brumberg <https://orcid.org/0000-0003-0959-4776>
 Valle Camacho <https://orcid.org/0000-0003-0748-0847>
 Daniel Alcolea <https://orcid.org/0000-0002-3819-3245>
 Rik Vandenberghe <https://orcid.org/0000-0001-6237-2502>
 Andrea Pilotto <https://orcid.org/0000-0003-2029-6606>
 Valentina Garibotto <https://orcid.org/0000-0003-2422-698X>

REFERENCES

- McKeith IG, Boeve BF, Dickson DW, *et al.* Diagnosis and management of dementia with Lewy bodies: Fourth consensus report of the DLB Consortium. *Neurology (Ecricon)* 2017;89:88–100.
- Rizzo G, Arcuti S, Copetti M, *et al.* Accuracy of clinical diagnosis of dementia with Lewy bodies: a systematic review and meta-analysis. *J Neurol Neurosurg Psychiatry* 2018;89:358–66.
- Surendranathan A, Kane JPM, Bentley A, *et al.* Clinical diagnosis of Lewy body dementia. *BJPsych Open* 2020;6:e61.
- Bousiges O, Blanc F. Biomarkers of Dementia with Lewy Bodies: Differential Diagnostic with Alzheimer's Disease. *Int J Mol Sci* 2022;23:6371.
- Agarwal K, Backler W, Bayram E, *et al.* Lewy body dementia: Overcoming barriers and identifying solutions. *Alzheimer's Dement* 2024;20:2298–308.
- Donaghy PC, Carrarini C, Ferreira D, *et al.* Research diagnostic criteria for mild cognitive impairment with Lewy bodies: A systematic review and meta-analysis. *Alzheimer's Dement* 2023;19:3186–202.
- McKeith IG, Ferman TJ, Thomas AJ, *et al.* Research criteria for the diagnosis of prodromal dementia with Lewy bodies. *Neurology (Ecricon)* 2020;94:743–55.
- Collij LE, Mastenbroek SE, Mattsson-Carlgrén N, *et al.* Lewy body pathology exacerbates brain hypometabolism and cognitive decline in Alzheimer's disease. *Nat Commun* 2024;15:8061.
- Diaz-Galvan P, Przybelski SA, Lesnick TG, *et al.* β -Amyloid Load on PET Along the Continuum of Dementia With Lewy Bodies. *Neurology (Ecricon)* 2023;101:101.
- Hamilton CA, Matthews FE, Donaghy PC, *et al.* Cognitive Decline in Mild Cognitive Impairment With Lewy Bodies or Alzheimer Disease: A Prospective Cohort Study. *Am J Geriatr Psychiatry* 2021;29:272–84.
- Brown RKJ, Bohnen NI, Wong KK, *et al.* Brain PET in suspected dementia: patterns of altered FDG metabolism. *Radiographics* 2014;34:684–701.
- Yamane T, Ikari Y, Nishio T, *et al.* Visual-statistical interpretation of (18)F-FDG-PET images for characteristic Alzheimer patterns in a multicenter study: inter-rater concordance and relationship to automated quantitative evaluation. *AJNR Am J Neuroradiol* 2014;35:244–9.
- Perovnik M, Vo A, Nguyen N, *et al.* Automated differential diagnosis of dementia syndromes using FDG PET and machine learning. *Front Aging Neurosci* 2022;14:1005731.
- Spetsieris PG, Eidelberg D. Scaled subprofile modeling of resting state imaging data in Parkinson's disease: methodological issues. *Neuroimage* 2011;54:2899–914.
- Perovnik M, Rus T, Schindlbeck KA, *et al.* Functional brain networks in the evaluation of patients with neurodegenerative disorders. *Nat Rev Neurol* 2023;19:73–90.
- Mattis PJ, Niethammer M, Sako W, *et al.* Distinct brain networks underlie cognitive dysfunction in Parkinson and Alzheimer diseases. *Neurology (Ecricon)* 2016;87:1925–33.
- Perovnik M, Tomše P, Jamšek J, *et al.* Identification and validation of Alzheimer's disease-related metabolic brain pattern in biomarker confirmed Alzheimer's dementia patients. *Sci Rep* 2022;12:11752.
- Tomše P, Jensterle L, Grmek M, *et al.* Abnormal metabolic brain network associated with Parkinson's disease: replication on a new European sample. *Neuroradiology* 2017;59:507–15.
- Perovnik M, Tomše P, Jamšek J, *et al.* Metabolic brain pattern in dementia with Lewy bodies: Relationship to Alzheimer's disease topography. *Neuroimage Clin* 2022;35:103080.
- Papathoma P-E, Markaki I, Tang C, *et al.* A replication study, systematic review and meta-analysis of automated image-based diagnosis in parkinsonism. *Sci Rep* 2022;12:2763.
- Nobili F, Festari C, Altomare D, *et al.* Automated assessment of FDG-PET for differential diagnosis in patients with neurodegenerative disorders. *Eur J Nucl Med Mol Imaging* 2018;45:1557–66.
- McKeith IG, Dickson DW, Lowe J, *et al.* Diagnosis and management of dementia with Lewy bodies: third report of the DLB Consortium. *Neurology (Ecricon)* 2005;65:1863–72.
- Arnold MR, Coughlin DG, Brumberg BH, *et al.* α -Synuclein Seed Amplification in CSF and Brain from Patients with Different Brain Distributions of Pathological

- α -Synuclein in the Context of Co-Pathology and Non-LBD Diagnoses. *Ann Neurol* 2022;92:650–62.
- 24 Ko JH, Lee CS, Eidelberg D. Metabolic network expression in parkinsonism: Clinical and dopaminergic correlations. *J Cereb Blood Flow Metab* 2017;37:683–93.
- 25 Ko JH, Katako A, Aljuaid M, et al. Distinct brain metabolic patterns separately associated with cognition, motor function, and aging in Parkinson's disease dementia. *Neurobiol Aging* 2017;60:81–91.
- 26 Brumberg J, Blazhenets G, Bühler S, et al. Cerebral Glucose Metabolism Is a Valuable Predictor of Survival in Patients with Lewy Body Diseases. *Ann Neurol* 2024;96:539–50.
- 27 Caminiti SP, Tettamanti M, Sala A, et al. Metabolic connectomics targeting brain pathology in dementia with Lewy bodies. *J Cereb Blood Flow Metab* 2017;37:1311–25.
- 28 Morbelli S, Chincarini A, Brendel M, et al. Metabolic patterns across core features in dementia with lewy bodies. *Ann Neurol* 2019;85:715–25.
- 29 Galli A, Pilotto A, Chiarini B, et al. Occipital atrophy signature in prodromal Lewy bodies disease. *Alzheimer's Dement Diagn Assess Dis Monit* 2023;15:1–5.
- 30 Caminiti SP, Sala A, Presotto L, et al. Validation of FDG-PET datasets of normal controls for the extraction of SPM-based brain metabolism maps. *Eur J Nucl Med Mol Imaging* 2021;48:2486–99.
- 31 Varrone A, Asenbaum S, Vander Borgh T, et al. EANM procedure guidelines for PET brain imaging using [18F]FDG, version 2. *Eur J Nucl Med Mol Imaging* 2009;36:2103–10.
- 32 Robin X, Turck N, Hainard A, et al. pROC: an open-source package for R and S+ to analyze and compare ROC curves. *BMC Bioinformatics* 2011;12:77.
- 33 Team P. RStudio: integrated development environment for R. 2024. Available: <http://www.posit.co/>
- 34 R Core Team. R: a language and environment for statistical computing. 2024. Available: <https://www.r-project.org/>
- 35 Wickham H. ggplot2. Cham: Springer International Publishing, 2016.
- 36 Woo C-W, Chang LJ, Lindquist MA, et al. Building better biomarkers: brain models in translational neuroimaging. *Nat Neurosci* 2017;20:365–77.
- 37 Iizuka T, Kameyama M. Spatial metabolic profiles to discriminate dementia with Lewy bodies from Alzheimer disease. *J Neurol* 2020;267:1960–9.
- 38 Lu J, Ge J, Chen K, et al. Consistent Abnormalities in Metabolic Patterns of Lewy Body Dementias. *Mov Disord* 2022;37:1861–71.
- 39 Carli G, Meles SK, Reesink FE, et al. Comparison of univariate and multivariate analyses for brain [18F]FDG PET data in α -synucleinopathies. *Neuroimage Clin* 2023;39:103475.
- 40 Katako A, Shelton P, Goertzen AL, et al. Machine learning identified an Alzheimer's disease-related FDG-PET pattern which is also expressed in Lewy body dementia and Parkinson's disease dementia. *Sci Rep* 2018;8:13236.
- 41 Kantarci K, Boeve BF, Przybelski SA, et al. FDG PET metabolic signatures distinguishing prodromal DLB and prodromal AD. *Neuroimage Clin* 2021;31:102754.
- 42 Mattioli P, Pardini M, Girtler N, et al. Cognitive and Brain Metabolism Profiles of Mild Cognitive Impairment in Prodromal Alpha-Synucleinopathy. *JAD* 2022;90:433–44.
- 43 Tang CC, Nakano Y, Vo A, et al. Longitudinal network changes and phenoconversion risk in isolated REM sleep behavior disorder. *Nat Commun* 2024;15:10797.
- 44 Carli G, Caminiti SP, Galbiati A, et al. In-vivo signatures of neurodegeneration in isolated rapid eye movement sleep behaviour disorder. *Euro J of Neurology* 2020;27:1285–95.
- 45 Lichter DG, Hershey LA. Proposal to Add FDG-PET as an Outcome Measure for Clinical Trials in Patients With Prodromal Lewy Body Dementia. *Neurology (Ecricon)* 2023;101:666–7.
- 46 Stockbauer A, Beyer L, Huber M, et al. Metabolic network alterations as a supportive biomarker in dementia with Lewy bodies with preserved dopamine transmission. *Eur J Nucl Med Mol Imaging* 2024;51:1023–34.
- 47 Tang CC, Poston KL, Eckert T, et al. Differential diagnosis of parkinsonism: a metabolic imaging study using pattern analysis. *Lancet Neurol* 2010;9:149–58.
- 48 Matar E, Halliday GM. Biological effects of pathologies in Lewy body diseases: why timing matters. *Lancet Neurol* 2025;24:441–55.
- 49 Robinson JL, Xie SX, Baer DR, et al. Pathological combinations in neurodegenerative disease are heterogeneous and disease-associated. *Brain (Bacau)* 2023;146:2557–69.
- 50 Kantarci K, Lowe VJ, Chen Q, et al. β -Amyloid PET and neuropathology in dementia with Lewy bodies. *Neurology (Ecricon)* 2020;94:e282–91.
- 51 Ishibashi K, Onishi A, Fujiwara Y, et al. Longitudinal effects of aging on 18 F-FDG distribution in cognitively normal elderly individuals. *Sci Rep* 2018;8:11557.
- 52 Chételat G, Arbizu J, Barthel H, et al. Amyloid-PET and 18F-FDG-PET in the diagnostic investigation of Alzheimer's disease and other dementias. *Lancet Neurol* 2020;19:951–62.
- 53 Zahirovic I, Wattmo C, Torisson G, et al. Prevalence of Dementia With Lewy Body Symptoms: A Cross-Sectional Study in 40 Swedish Nursing Homes. *J Am Med Dir Assoc* 2016;17:706–11.
- 54 Heybe M, Gibson L, Price AC, et al. Identifying people with potentially undiagnosed dementia with Lewy bodies using natural language processing. *NPJ Aging* 2025;11:68.
- 55 Ge J, Wu J, Peng S, et al. Reproducible network and regional topographies of abnormal glucose metabolism associated with progressive supranuclear palsy: Multivariate and univariate analyses in American and Chinese patient cohorts. *Hum Brain Mapp* 2018;39:2842–58.
- 56 Tomšič P, Peng S, Pirtošek Z, et al. The effects of image reconstruction algorithms on topographic characteristics, diagnostic performance and clinical correlation of metabolic brain networks in Parkinson's disease. *Phys Med* 2018;52:104–12.
- 57 Tomšič P, Jensterle L, Rep S, et al. The effect of 18F-FDG-PET image reconstruction algorithms on the expression of characteristic metabolic brain network in Parkinson's disease. *Phys Med* 2017;41:129–35.
- 58 Štokelj E, Tomšič P, Tomanič T, et al. Effect of the identification group size and image resolution on the diagnostic performance of metabolic Alzheimer's disease-related pattern. *EJNMMI Res* 2023;13:47.